The Astrophysical Journal, 677:L129–L132, 2008 April 20

EVIDENCE FOR WIND-LIKE REGIONS, ACCELERATION OF SHOCKS IN THE DEEP CORONA, AND RELEVANCE OF 1/*f* DYNAMIC SPECTRA TO CORONAL TYPE II BURSTS

V. V. Lobzin, Iver H. Cairns, and P. A. Robinson
School of Physics, University of Sydney, Sydney, NSW 2006, Australia; v.lobzin@physics.usyd.edu.au
Received 2008 January 23; accepted 2008 March 4; published 2008 March 26

ABSTRACT

Type II radio bursts are produced near the local plasma frequency f_p and near $2f_p$ by shocks moving through the corona and solar wind. In the present Letter eight well-defined coronal type II radio bursts (30–300 MHz) are analyzed. Three results are presented. First, it is found that the dependence of the central frequency on time can be fitted to a power-law model, $f \propto (t - t_0)^{-\alpha}$, with $0.6 \leq \alpha \leq 1.3$. Assuming a constant shock velocity, these results provide evidence that the density profile $n_e(r)$ in the type II source regions closely resembles the solar wind, with $n_e(r) \propto r^{-2}$. One possible interpretation is that the solar wind starts within a few solar radii of the photosphere, most probably within 1 solar radius. Another relies on a gasdynamic Whitham analysis and demonstrates a possibility for blast shocks to accelerate, thereby reducing apparent power-law indices to solar wind–like values. Second, for the events considered it is found that radio burst emission in the form of 1/*f* versus *t* dynamic spectra closely follows straight lines. In future this will allow much more objective identification of type II bursts in solar radio data and plausibly real-time correlation with coronagraph and other solar radar. Third, it is demonstrated that 1/*f* versus *t* dynamic spectra can provide direct evidence for acceleration of the shock deep in the corona, thus complementing coronagraph studies.

Subject headings: shock waves — solar wind — Sun: corona — Sun: radio radiation

1. INTRODUCTION

Coronal type II bursts were discovered in the early 1950s in the frequency range 40–240 MHz and quickly interpreted in terms of radio emission produced near the local plasma frequency f_p and near $2f_p$ in association with shock waves (Wild & McCready 1950). Analogous interplanetary radio emissions were discovered later (Cane et al. 1982). Both coronal and interplanetary type II bursts are now interpreted in terms of electron acceleration at a fast-mode shock and the subsequent formation of electron beams, Langmuir waves, and then f_p and $2f_p$ radiation in foreshock regions upstream of the shock. This basic picture is supported by in situ (Bale et al. 1999) and remote observations (Reiner et al. 1998) and a detailed theory (Knock et al. 2001; Knock & Cairns 2005; Florens et al. 2007) that shows qualitative agreement with experimental data.

Since f_p is proportional to the square root of the electron number density n_e, the dynamic radio spectra for both type II and III radio bursts can be used to estimate the coronal plasma density and study the dynamics of the emission source. A common approach is to choose a particular coronal/solar wind density model and then obtain a height-time diagram showing the source dynamics. Conversely, assuming that the radio source is moving with a constant speed, one can deduce the profile of n_e. In the solar wind Kellogg (1980), Reiner et al. (1998), and others realized that a shock moving with constant speed through the solar wind plasma with $f_p(r) \propto r^{-1}$ and producing radiation at $f_p(t)$ and $2f_p(t)$ would result in straight lines in dynamic spectra for which $1/f(t)$ is plotted against t (here and below r is the radial distance from the Sun in units of the solar radius, $R_\odot$). This technique is used in identifying interplanetary type II bursts, the slowing of interplanetary shocks, and predicting the arrival time of type II shocks and accompanying CMEs at Earth.

It is generally accepted that the density distribution in the solar corona, where the meter-wavelength bursts originate, is considerably more complicated and has a much steeper density falloff than in the solar wind. Leblanc et al. (1998) derived the electron density distribution in the ecliptic plane, from the corona to 1 AU,

$$n_e(r) = 3.3 \times 10^{11} r^{-2} + 4.1 \times 10^{12} r^{-4} + 8.0 \times 10^{13} r^{-6} \ \mathrm{m}^{-3}. \quad (1)$$

From equation (1) it follows that for small distances, $r \lesssim 3$, the density scales as $n_e \propto r^{-6}$, while for larger distances, $r \gtrsim 7$, we have $n_e \propto r^{-2}$. Leblanc et al. (1998) argue that model (1) represents electron densities from the solar corona ($r \simeq 1.8$) to 1 AU. However, close to the Sun the gradients are supposed to be much steeper. Indeed, the Baumbach-Allen density distribution (Allen 1947), which is expected to be valid in the range $1 \lesssim r \lesssim 2.6$, is given by

$$n_e(r) = 10^{14}(1.55 r^{-6} + 2.99 r^{-16}) \ \mathrm{m}^{-3}. \quad (2)$$

The density models (1) and (2) suggest that the technique of plotting 1/*f* versus *t* will not be useful for solar bursts originating in corona. To the best of our knowledge, no one has previously demonstrated the usefulness of 1/*f* versus *t* dynamic spectra for coronal type II bursts.

The aims of the Letter are threefold. First, to demonstrate that quantitative study of the frequency-time profiles of eight well-defined type II bursts provides strong evidence that the density profile $n_e(r)$ in the type II source regions closely resembles that of the solar wind. Second, to show that 1/*f* versus *t* dynamic spectra are often directly relevant to coronal type II bursts, which produce closely straight-line signatures in these plots. In future this will enable much more objective identification of type II bursts in solar radio data and plausibly real-time correlation with coronagraph and other solar data. Third, to demonstrate that the 1/*f* versus *t* dynamic spectra can provide direct evidence for acceleration of the driving shock deep in the corona, thereby complementing coronagraph studies. These aims are accomplished by describing the solar radio observa-

TABLE 1
RESULTS OF POWER-LAW FITTING FOR TYPE II SPECTRA

Number	Date	Band[a]	Analyzed Time Interval (UT)	Frequency Range (MHz)	α
1	2001 Sep 3	H	01:58:41–02:02:35	53.3–83.9	0.56 ± 0.13
2	2000 Sep 9	H low	08:42:33–08:47:03	81.3–117.3	0.67 ± 0.08
3	2002 Jan 25	H low	02:27:30–02:37:30	70.4–129.1	0.58 ± 0.05
3	2002 Jan 25	F high	02:27:33–02:37:21	42.3–78.9	0.48 ± 0.05
4	2002 Aug 23	H	05:49:17–05:55:32	85.0–153.0	0.80 ± 0.10
5	2002 Oct 4	F low	22:46:50–22:56:35	34.4–62.0	0.99 ± 0.09
5	2002 Oct 4	F high	22:45:59–22:54:44	42.9–93.9	0.73 ± 0.04
5	2002 Oct 4	H high	22:47:32–22:55:17	80.3–140.4	1.3 ± 0.2
5	2002 Oct 4	H low	22:46:02–22:55:08	70.8–132.8	1.00 ± 0.12
6	2003 May 31	H	02:26:37–02:32:04	55.3–117.3	0.67 ± 0.08
7	2003 Oct 26	F	06:17:03–06:19:00	54.4–87.1	1.1 ± 0.5
8	2006 Dec 14	H	22:11:54–22:15:15	78.4–147.7	0.58 ± 0.09

[a] F and H correspond to fundamental and harmonic emission, respectively.

tions, analyses, and results (§ 2), interpreting and discussing the results (§ 3), and then giving the conclusions (§ 4).

2. OBSERVATIONS, DATA ANALYSES, AND RESULTS

Using event listings provided by NOAA's National Geophysical Data Center, we have examined type II events observed at Learmonth Observatory from year 2000 up to now. The Learmonth solar radio spectrograph covers a frequency range of 25–180 MHz in two bands, completing a sweep every 3 s. For further analysis we selected eight events with the following characteristics: (1) upper frequency $\geq$ 150 MHz, (2) intensities of 2 or 3, (3) the event is definitely a type II burst with clear bands corresponding to both fundamental and harmonic emissions. The list of the events chosen is presented in Table 1. The dynamic spectrum for one selected event is shown in Figure 1.

To describe the frequency drift of the type II bursts quantitatively, we choose a band of interest, then for each time t_i we find the frequency f_i of maximum signal strength. The dynamic spectrum in Figure 1 clearly shows the solar radio emission and many interference lines related to communications systems, ionosondes, etc. When the maximums f_i are obviously strongly affected by interference, the corresponding data points are discarded. The next stage of data processing is fitting the measured frequencies f_i to a model that depends on adjustable parameters. The frequencies f_i usually do not lie on a smooth curve. Rather, they show considerable fluctuations that can be attributed to measurement errors. Since such errors are unlikely to be normally distributed and obviously result in outliers, least-squares fitting is inappropriate. Instead, we use a robust technique of minimizing the mean absolute deviation, $X^2 = \sum_i (|f - f_i|/\sigma_i)$,where f is the frequency predicted by the model and σ_i is the estimate of error for given time and frequency.

To find a suitable model function $f = f(t)$, suppose that the source of the emission starts from position r_0 at time t_0 with initial speed v_0 and constant acceleration a_0. Then $r(t) = r_0 + v_0(t - t_0) + a_0(t - t_0)^2/2$. With $f_p(r) \propto r^{-\alpha}$, if the source produces radio emission at a time-varying frequency $f(t) = mf_p(r(t))$, where $m = 1$ for fundamental and $m = 2$ for harmonic emission, then $f(t) = mA\,[r_0 + v_0(t - t_0) + a_0(t - t_0)^2/2]^{-\alpha}$. If we assume further that the effect of acceleration is negligible for the time interval considered, this reduces to

$$f(t) = a(t - b)^{-\alpha}, \tag{3}$$

where a and b are constants related to A, t_0, r_0, and v_0. Thus, by fitting the time-varying radiation frequency to model (3), the power-law index (-2α) for the local density profile can be obtained independent of v_0 or the absolute scale of r. The power of this approach does not appear to have been appreciated previously. Instead, previous studies analyzed the frequency drift rates df/dt versus f, assuming an absolute scale for $n(r)$ or else a distance scale to study the dynamics of the radiation source (e.g., Warmuth & Mann 2005).

The results of fitting are summarized in Table 1. The errors for α are estimated as $(P_{87.5} - P_{12.5})/2$, where P_k denotes the kth percentile; thus, the probability for α to fall into the corresponding interval is about 75%. Figure 2 plots $f(t)$ versus t

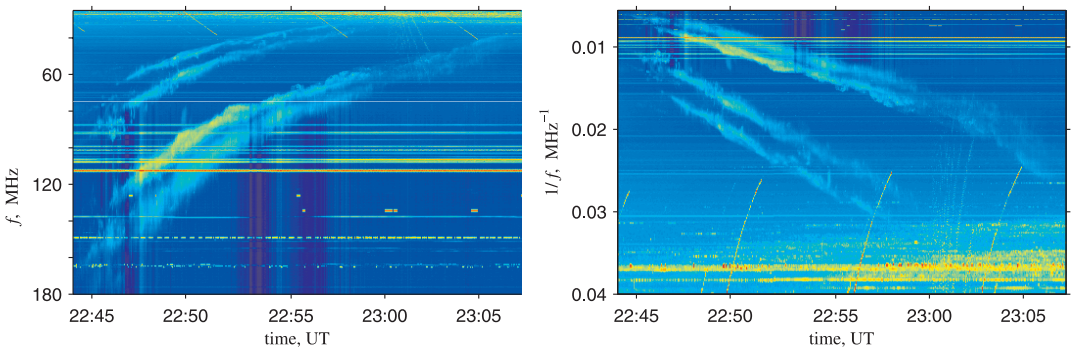

FIG. 1.—(*Left*) Dynamic spectrum of the split-band type II burst (event 5) beginning at 2002 October 4, 22:44 UT. (*Right*) $1/f$ vs. t dynamic spectrum for the same event. Clearly visible within the time interval 22:46–22:59 are four nearly straight type II lanes. Then, after a gap, the slope of the harmonic emission lane increases considerably.

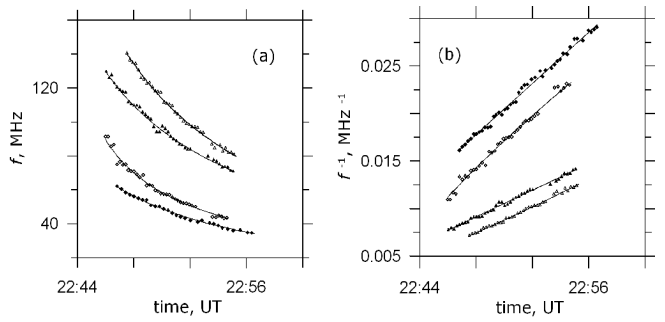

FIG. 2.—Plots of (*a*) frequencies corresponding to maximum intensity, $f(t)$, and (*b*) $1/f(t)$ vs. time. Superposed lines correspond to best power-law fits for each lane of event 5.

with the fit lines superposed for event 5 presented in Figure 1. Importantly, each pair of fundamental and harmonic bands for a given event yields the same result for α to within the error bars, consistent with the radiation being fundamental and harmonic emission from an object moving through a single density profile.

The primary result of Figures 1 and 2 and Table 1 is that the sources of all eight type II bursts in our data set seem to be moving through regions of the corona in which the density is surprisingly slowly changing, with $0.6 \leq \alpha \leq 1.3$ and an average 0.8 ± 0.3, very similar to that of the solar wind.

The finding that $\alpha \simeq 1$ suggests that plotting $1/f(t)$ versus t will yield an approximately straight line in dynamic spectra. Figure 1 demonstrates this for event 5. Moreover, all the eight type II events studied here yield long-lived approximately linear bands in $1/f$ versus t dynamic spectra. Thus, $1/f$ versus t dynamic spectra are unexpectedly useful in identifying coronal type II bursts.

3. INTERPRETATIONS AND DISCUSSION

Each radio burst frequency is indicative of the distance between its source and the Sun. From the density models (1) and (2) it follows that frequencies of 150 and 20 MHz correspond to heliocentric distances of 1.04 $R_\odot$ and 1.6 $R_\odot$, respectively.

Important implications follow from finding that the selected coronal type II events have frequency-time profiles consistent with f_p and $2f_p$ radiation generated near a shock moving at approximately constant speed through coronal regions with density profiles $n_e(r) \propto r^{-1.6\pm0.5}$. At least two different kinds of explanations of these observations could be suggested. The explanations of the first kind imply that the source speed does not change considerably in the region of interest, while the explanations of the second kind presume that the shock dynamics is not so trivial.

First, assume that the shock speed varies relatively slowly and, as a consequence, the real density profile is close to $n_e(r) \propto r^{-2}$. The most direct interpretation is that these regions, with solar wind–like density profiles and sizes of order a fraction of a solar radius ($\Delta r \simeq 300$ s × 1000 km s^{-1} = 3 × 10^8 m), are indeed regions of the solar wind. Should this be the case, the coronal models (1) and (2) for $f_p(r)$ imply that some regions of the solar wind do form within a few solar radii of the photosphere, most probably within 1 solar radius. Unfortunately, absolute measurements of the source position for the bursts considered are not available, so this conclusion relies on previous density models.

An alternative interpretation of the inferred solar wind–like density profiles is that the type II shock is riding over an enhanced outflow of plasma, presumably from active portions of the photosphere and low corona, whose number density is decaying approximately as r^{-2} due to number conservation but dominates the standard coronal density profile. The widely different onset times of type II bursts, CMEs, and flares suggests that this outflow should be relatively long-lived, with significant time required to set up a relatively steady r^{-2} profile.

Figure 1 and analogs show that $1/f$ versus t dynamic spectra should be unexpectedly useful for identifying type II bursts in coronal density data. Hough transforms should thus enable objective and automatic type II identification and analysis, as done for CME data by Robbrecht & Berghmanns (2004).

For negligible source acceleration, the slope in $1/f$-t space is proportional to v_0. Accordingly, deceleration of a shock will lead to a $1/f$-t band that becomes more horizontal, whereas an increase in speed (positive acceleration) will lead to steepening. Thus, acceleration should cause curving of the emission band away from a linear $1/f$-t trend. This effect could also result from a change in the power-law index of the density profile. Reconsidering Figure 1 in this context, the existence of linear $1/f$-t bands at early and late times but with different slopes provides direct evidence for acceleration of the shock in the corona (between the two intervals with linear bands), because the linear bands correspond to regions where $n_e \propto r^{-2}$ and the larger slope at later times corresponds to larger shock speed.

Although the interpretation involving shocks moving with approximately constant speed seems to be the most straightforward, alternative explanations cannot be excluded at this stage. In particular, consider briefly an interpretation that assumes shocks do not move with a constant speed in the solar corona. The shocks could accelerate or decelerate depending on several factors, including the local density profile and geometrical aspects of the shock propagation. Indeed, it is known that the speeds of gasdynamic shocks do vary in similar situations. In particular, planar shocks moving against a density gradient are accelerated (see, e.g., Zel'dovich & Raizer 1967). Similarly, Sedov (1959) studied the problem of strong spherical explosion into a medium whose density ρ decreases with the distance according to $\rho \propto r^{-\omega}$: self-similar solutions with the shock position given by $r \propto t^{\alpha}$ were found, with the shocks decelerating if $\omega < 3$ and accelerating if $\omega > 3$.

It is unlikely that these self-similar solutions are directly applicable to the solar corona, since MHD theory is likely more relevant than gasdynamics. In addition, these self-similar solutions were derived under rather restrictive symmetry conditions. More general cases, with both moving media and arbitrary density profiles, can be analyzed using the approximate method developed by Whitham (1974).

We next use Whitham's approach to demonstrate that accelerating shocks can produce spectrograms with approximately linear $1/f$ versus t dependencies. To do this we assume that the plasma flow obeys the Parker (1958) model with a polytropic equation of state with index γ and the shock speed is high enough to allow us to simplify the Rankine-Hugoniot relations and to neglect the plasma speed ahead of the shock and the effect of solar gravitation on the shock dynamics (the gravity still causes the plasma stratification). If the plasma density approximately obeys $\rho \propto r^{-\omega}$ with $\omega > 0$, then Whitham's approach leads to power-law dynamics of the shock wave,

$$r(t) \propto \frac{1}{(-t)^{1/(\beta-1)}},$$

with $\beta = [\omega - 4/(2 + y)]y/2$ and $y = [2\gamma(\gamma - 1)]^{1/2}$. Here it is assumed that $t < 0$ and $r \to +\infty$ as $t \to -0$. This shock accelerates outward, and since $f_p(r) \propto r^{-\omega/2}$, we find

$$f(t) \propto (-t)^{\xi},$$

where

$$\xi = \frac{\omega}{2(\beta - 1)}.$$

If we take $\omega = 6$, in accordance with coronal models (1) and (2), ξ can be as low as 1.1 for $\gamma = 5/3$.

Thus, although the model used to obtain these estimates is definitely oversimplified, it is able to demonstrate qualitatively that acceleration of shocks moving against steep density gradients in the solar corona could produce type II radio bursts with relatively slow frequency drift. More quantitative investigation of this problem is beyond the scope of the present Letter and will be addressed in the future.

Finally, we note that these $f(t)$ analyses and $1/f$ versus t dynamic spectra may be useful for type III bursts as well. Indeed, combining theoretical results with observations of type III bursts in the range 10 kHz to 10 MHz corresponding to heliocentric distances from ~1 AU to ~2.1 $R_\odot$, Robinson & Cairns (1998) found $n_e(r) \propto (r - 1)^{-2.19 \pm 0.05}$. The Learmonth data analyzed here have insufficient time resolution to be relevant to type III bursts. To obtain quite reliable fits of observed frequencies, it is desirable to have 200–300 measurements for each event. For type III bursts with a typical duration of 1–3 s, the corresponding time resolution should be of the order of 10 ms. Data from the 32 tile phase of the Murchison Widefield Array (MWA) will be suitable to test the type II results.

4. CONCLUSIONS

The present study used the solar radio data from 25 to 180 MHz with time resolution of 3 s from Learmonth Solar Radio Observatory in Australia. Eight well-defined type II radio bursts were analyzed. For these events it was found that the dependence of the central frequency on time is well fitted by a power-law model, $f \propto (t - t_0)^{-\alpha}$, with $0.6 \leq \alpha \leq 1.3$. The most direct interpretation of these results, assuming an approximately constant shock speed, is that the density profile $n_e(r)$ in the type II source regions closely resembles the solar wind, $n_e(r) \propto r^{-1.6 \pm 0.5}$. Thus the solar wind could start within a few solar radii of the photosphere, most probably within 1 solar radius. Alternatively, the shock may ride over an enhanced plasma outflow, with $n_e(r) \propto r^{-2}$ from mass conservation, rather than the ambient corona. A qualitatively different interpretation presumes that the shock speed can change rapidly, thereby influencing the observed frequency drift. A gasdynamic Whitham analysis demonstrates qualitatively that a blast wave shock can accelerate outward in a way that can reduce the apparent density index α to solar wind–like values. Further research on these interpretations is required.

Since the power-law index α is close to unity for the events considered, radio burst emissions in $1/f$ versus t dynamic spectra resemble straight lines. In future this will allow much more objective and efficient identification of type II bursts in solar radio data and plausibly real-time correlation with coronagraph and other solar instruments. In addition, it was demonstrated that the $1/f$ versus t dynamic spectra can provide direct evidence for acceleration of the driving shock deep in the corona, thereby complementing coronagraph studies.

We thank our colleagues D. Cole, G. Patterson, G. Steward, and P. Wilkinson from IPS Radio and Space Services for helpful discussions and the Australian Research Council for funding.

REFERENCES

Allen, C. W. 1947, MNRAS, 107, 426
Bale, S. D., Reiner, M. J., Bougeret, J.-L., Kaiser, M. L., Krucker, S., Larson, D. E., & Lin, R. P. 1999, Geophys. Res. Lett., 26, 1573
Cane, H. V., Stone, R. G., Fainberg, J., Steinberg, J. L., & Hoang, S. 1982, Sol. Phys., 78, 187
Florens, M. S. L., Cairns, I. H., Knock, S. A., & Robinson, P. A. 2007, Geophys. Res. Lett., 34, L04104
Kellogg, P. J. 1980, ApJ, 236, 696
Knock, S. A., & Cairns, I. H. 2005, J. Geophys. Res., 110, A01101
Knock, S. A., Cairns, I. H., Robinson, P. A., & Kuncic, Z. 2001, J. Geophys. Res., 106, 25041
Leblanc, Y., Dulk, G. A., & Bougeret, J.-L. 1998, Sol. Phys., 183, 165
Parker, E. N. 1958, ApJ, 128, 664
Reiner, M. J., Kaiser, M. L., Fainberg, J., & Stone, R. G. 1998, J. Geophys. Res., 103, 29651
Robbrecht, E., & Berghmans, D. 2004, A&A, 425, 1097
Robinson, P. A., & Cairns, I. H. 1998, Sol. Phys., 181, 429
Sedov, L. I. 1959, Similarity and Dimensional Methods in Mechanics (New York: Academic)
Warmuth, A., & Mann, G. 2005, in Space Weather, ed. K. Scherer et al. (Berlin: Springer), 51
Whitham, G. B. 1974, Linear and Nonlinear Waves (New York: Wiley)
Wild, J. P., & McCready, L. L. 1950, Australian J. Sci. Res. A, 3, 387
Zel'dovich, Ya. B., & Raizer, Yu P. 1967, Physics of Shock Waves and High-Temperature Hydrodynamic Phenomena, Vol. 2 (New York: Academic)